Journal of Engineering Science and Technology Review 15 (5) (2022) 52 - 61

Research Article

JOURNAL OF
Engineering Science and Technology Review

www.jestr.org

Mechanical Response Analysis of Asphalt Pavement Based on the Interlayer Contact State between Cement-stabilized Magnesium Slag–Aeolian Sand Base

Changfeng Sun [1], Jiahao Zhang [2, 3, *], Xin Yang [1], Meng Gao [4, 5] and Hongjun Jing [4, 5]

[1] YuLin Highway Bureau, Yulin 719000, China
[2] CCCC Second Highway Engineering Bureau Co., Ltd, Xi'an 710065, China
[3] Research and Development Center on Construction Technology of Long Bridge and Tunnel in Mountain Areas, CCCC, Xi'an 710199, China
[4] College of Architecture and Civil Engineering, Xi'an University of Science and Technology, Xi'an 710054, China
[5] Road Engineering Research Center, Xi'an University of Science and Technology, Xi'an 710054, China

Received 19 June 2022; Accepted 12 November 2022

Abstract

In this study, a 3D finite element model was established for the asphalt pavement with cement-stabilized magnesium slag–aeolian sand base to explore the difference between the performance of cement-stabilized magnesium slag–aeolian sand base under the actual operation state and that under the design operation state. The model was also used to provide a theoretical basis for determining their construction technologies and the causes of pavement damage. Moreover, it was used to simulate the three-layer continuous, layered continuous, and layered discontinuous construction technologies through the interlayer contact state between bases (upper base, lower base, and subbase). Next, under the action of traffic load, the mechanical response of this model under the completely continuous state and three construction technologies was calculated. On this basis, the influence of the interlayer contact state between bases on the mechanical response of structural layers in the asphalt pavement was analyzed. Results demonstrate that in case of the change in the interlayer contact state between bases, the vertical displacement on the surface of each structural layer basically keeps an unchanged distribution, and the horizontal compressive stress at the bottom of the upper base is turned into tensile stress, and the maximum shear stress at the bottom of the lower base is changed from a smooth bimodal distribution into a unimodal distribution. The index values are influenced to different degrees, among which the horizontal tensile stress at the bottom of the upper and lower bases is influenced to the greatest extent, followed by the maximum shear stress at the bottom of the upper base, lower base, and subbase and the vertical displacement of the pavement. When the layered continuous and discontinuous construction technologies are adopted, the pavement performance index decrease by 3.0% and 6.5%, respectively, in comparison with that in the event of layered continuous construction technology. The layered continuous construction technology is recommended, and pertinent measures should be taken during the construction stage.

Keywords: Road engineering, Interlayer contact between base, Cement-stabilized magnesium slag–aeolian sand base, Finite element analysis, Construction technology

1. Introduction

Mineral resources have played a vital role in China's modernization construction and economic development, but they are relatively collectively distributed in China. The construction of road transportation infrastructure should be continuously updated and perfected to ensure reasonable resource allocation and drive balanced regional economic development, so the demands for soil and stone resources have been gradually growing. However, the long-term exploitation of natural soil and stones will seriously destruct the mountain ecology and pollute the environment [1]. Meanwhile, the price of natural soil and stones is continuously rising due to their nonuniform distribution and the prohibition of disordered mining in China, which will seriously restrict the highway construction speed. In recent years, China has started a green transformation to improve the national economic level [2], so highway construction should not be restricted to conventional materials under this background.

The main magnesium smelting technology in China is the Pidgeon method—a world magnesium production base, and about 5–6 t of magnesium slags will be discharged by producing every 1 t of magnesium metal [3]. In Yulin City, China, for example, the annual discharge of magnesium slags exceeds 3,000,000 t. At present, magnesium slags are disposed mainly by means of stacking and burying. If buried in soil, magnesium slags whose main chemical components are CaO, SiO_2, and MgO [4] will react with water [5], which causes soil consolidation and seriously harms the normal growth of animals and plants. If arbitrarily piled up, magnesium slags will waste plenty of lands and pollute the atmospheric environment. Recycling magnesium slags to maintain the sustainable development of the magnesium industry is already inevitable. The Maowusu Desert in this territory is one of the four major deserts in China [6], with typical aeolian sand landforms. In comparison with stone materials needing transportation from other places, the aeolian sand resources can be locally obtained, which, if reasonably exploited, will not destruct the ecology, thereby possessing broad application prospects in pavement engineering.

*E-mail address: zjh1223292484@163.com
ISSN: 1791-2377
doi:10.25103/jestr.155.08

Therefore, one of the effective paths to solving the shortage of road construction materials and the disposal difficulty of magnesium slags lies in taking cement-stabilized magnesium slag–aeolian sand mixture as the new base material. The practical pavement performance of new materials is a factor in deciding whether they can be promoted and applied. In the current design code for asphalt pavement in China, the elastic layered system theory is adopted in the structural design and checking calculation of cement-stabilized base. Bases are regarded as a whole, but layered construction technology is generally preferred for thick cement-stabilized bases. Influenced by factors such as the environment and construction quality during the construction, however, the interlayer contact state between bases becomes poor, leading to the inconformity of the actual bonding state of pavement structural layers with the design operation state and further giving rise to early pavement diseases [7].

Given the above problems, the cement-stabilized magnesium slag–aeolian sand mixture was used as the new base material of pavements to explore its mechanical response when applied to practical projects through different construction technologies. Moreover, construction technologies were optimized to ensure that the new material could exert good pavement performance in practical engineering. In this manner, the new material was transformed from the research project into practical application, thereby creating broad application prospects.

2. State of the art

When arbitrarily stacked, industrial waste slags, such as magnesium slags, will not only generate irreversible influences on the ecological environment but also waste their resource utilization values [8]. Hence, scholars from various countries have investigated the application of industrial waste slags to roads and tried their engineering applications. Karatag et al. [9] comparatively studied the pavement performance of steel slags and macadams, and proved that steel slags are applicable to pavement base and subbase. In view of the environmental problem brought by the difficulty in disposing of coal gangues, Ashfaq et al. [10] stabilized coal gangues with lime, explored the change laws of their unconfined compressive strength, and finally proved the good pavement performance of coal gauges in pavement base and subbase. Gonawala et al. [11] studied arc furnace slag–15% blast furnace slag mixture as the base material of pavements. They discovered that the strength of this mixture meets the base course requirements of rural roads and can serve as a harmless road construction material for roads with low traffic volumes. Pires et al. [12] probed the applicability of steel slag stabilized soil as the base material of pavements, and found that inferior soil stabilized by 20% desulfurized steel slag had equivalent performance to 3% cement-stabilized superior soil, displaying excellent pavement performance. Some scholars have doubted the environmental safety of industrial waste slags if applied to pavements. Hence, Reinik et al. [13] conducted long-term environmental toxicity monitoring of an oil shale road construction project, and discovered that no hazardous substances leached out and polluted the surrounding environment. With industrial ferronickel slags as the study objects, He et al. [14] explored their applicability as subgrade fillings, and found that the fillers showed better engineering applicability and could be directly used to fill the subgrade with minor environmental pollution after 10%–20% of clay was added. As early as the last century, Huang et al. [15] proposed using lime–ash-stabilized magnesium slags as new base materials of pavements in sand-free areas in northeast China, and achieved significant socioeconomic benefits. However, magnesium slags as base materials of pavements have been scarcely explored due to their powdery shape and expansibility. At present, the paths to resource utilization of magnesium slags mainly include calcination of cement clinker [16], asphalt modification [17], and application as cementing materials [18], with low recycling efficiency. Moreover, lime–ash-stabilized magnesium slags can no longer adapt to the current traffic flow and traffic loads. Conversely, the application of aeolian sands to pavements has been extensively investigated considering their engineering characteristics, such as high modulus of compression and favorable compaction. Song et al. [19] performed a series of indoor experiments and engineering applications to use aeolian sands to semirigid base courses. They found that after aeolian sands replaced the fine aggregates in cement-stabilized macadam, the performance of aeolian sands was gradually degraded with the increase in the replacement ratio, the maximum of which was finally recommended to be 6%. Al-Taie et al. [20] explored the engineering characteristics of aeolian sands in Baig City in Iraq, and proved the good applicability of aeolian sands in this area to road engineering. They also established the technical standard for cement-stabilized aeolian sand materials according to their mechanical properties. However, the utilization rate of aeolian sands is low in the abovementioned studies. In addition, cement-stabilized aeolian sands are only applicable to the subbase of pavements due to their poor mechanical properties. Little efforts have been made to comprehensively use aeolian sands and industrial solid wastes in pavement bases in areas rich in mineral and desert resources.

Zhang et al. [21] solidified electrolytic manganese slags, red mud, and carbide slags, and explored their pavement performance based on the synergistic effect of multiple materials. This study provides a new idea for the comprehensive utilization of multiple materials, that is, the good synergistic effect of materials can contribute to excellent constitutive properties of base course materials. Under the application status of the abovementioned magnesium slags and aeolian sands in pavements, the cement-stabilized magnesium slag–aeolian sand base material was experimentally studied [22] by the research group based on the research idea of the comprehensive utilization of multiple materials, and the good pavement performance of the mixture, as a new base course material, was proved. However, given the great differences among magnesium slags, aeolian sands, and conventional road construction materials in material properties, the mix design and pavement performance research regarding the cement-stabilized magnesium slag–aeolian sand mixture cannot sufficiently guarantee that it can exert good stability in high-grade pavements or large-scale projects. The layered construction technology has been mostly applied to base at present. Influenced by environmental factors and inefficient quality control during construction, the cohesiveness between base, however, becomes poor, leading to the inconformity of the actual bonding state of pavement structural layers with the design state. The influencing laws and influencing degree of the interlayer contact state between bases on the pavement performance of cement-stabilized magnesium slag–aeolian sand bases should be explored to improve the promotion and utilization value.

Hwang et al. [23] simulated the bonding failure between bituminous and cement concrete, characterized the shear strength of pavements using clamping shear strength, and finally explained the texture effect of the bonding behaviors between bases. Mazurek et al. [24] simulated the interaction between pavement structural layers through a cohesive contact model. They concluded that the large deformation of the pavement structure would result in the loss of aggregate particles in the base course made of recycled materials, as well as many cracks at the edge of the road structure. Saannibe et al. [25] probed the influence of milk lime, which was spread on the bonded coating, on the bonding strength between structural layers of the asphalt pavement. They found that the bonding strength between structural layers was significantly enhanced by the bonded coating or bonded coating + milk lime in comparison with the situation of unbonded coating. Spadoni et al. [26] studied the influences of the composites of four geotechnical materials with asphalt on the interlayer bonding and the crack propagation of asphalt pavements. They found that geotechnical composites can delay the reflective cracking to lengthen the service life of pavements; however, these composites deteriorate the bonding state between asphalt surfaces. Wang et al. [27] established an interlayer contact model to simulate the bonding and bonding failurestatus between adjacent structural layers of asphalt pavement with semirigid base courses and analyzed the mechanical response of structural layers at room and high temperatures. They discovered that the mechanical properties of the asphalt pavement would be deteriorated due to the separation of surface and base, which is especially prominent at high temperatures, and the pavement is deteriorated more greatly by moving loads than the subgrade at high temperatures. Wu et al. [28] simulated the interlayer contact state between the semirigid base and asphalt surface through the flexibility of shear spring and explored the influences of different interlayer bonding conditions and the thickness of the surface on the mechanical response. The results showed that when the interlayer contact state is turned from a complete bonding state into a complete smooth state, the variation range of the maximum shear stress is the greatest, whereas that of the deflection is the minimum. To sum up, most of the existing studies have focused on the interlayer contact state between base and surface, whereas the influence of the interlayer contact state between semirigid bases on the mechanical response of pavements has been insufficiently involved. In addition, the construction technology of bases has rarely been simulated through the interlayer contact state between bases.

Therefore, the pavement performance of cement-stabilized magnesium slag–aeolian sand mixtures was explored, considering the experience and deficiencies of existing studies. On this basis, the interlayer contact state of cement-stabilized magnesium slag–aeolian sand bases and the three construction technologies were simulated through the interlayer contact state among upper base, lower base, and subbase via finite element software ABAQUS in this study. Moreover, the influence of the interlayer contact state between bases on the mechanical response of the asphalt pavement under the action of traffic loads was analyzed. Accordingly, the base construction technologies were optimized to provide a theoretical basis for determining the construction technology and key technologies for cement-stabilized magnesium-aeolian sand bases and expand the application and promotion prospects of such base materials.

The remainder of this study is organized as follows. In Section 3, the contact theory and the finite element modeling method of pavements adopted in finite element simulation were expounded. In Section 4, the calculation results for the mechanical response of pavements were analyzed, followed by the optimal selection of construction technologies. In the final section, the related conclusions were presented.

3. Methodology

In this study, the simulation method for the three construction technologies based on the interlayer contact state among the surface, base, and subbase via ABAQUS was given. Next, the road structure, material parameters, load form, mechanical response analysis indexes, and extraction path were determined. On this basis, a 3D finite element model of the asphalt pavement with cement-stabilized magnesium slag–aeolian sand bases was established, and the influences of different construction technologies on the mechanical response of structural layers were analyzed. Finally, the construction scheme was optimally selected.

3.1 Contact theory of pavement structural layers

At present, the mechanical response of pavements has been calculated mostly according to the standards currently in force. The pavement structures are regarded as a whole, without an interlayer relative slip. However, the base is generally paved in two separate layers—upper and lower bases—in practical engineering. A weak structural layer will be formed between the upper and lower bases, and its mechanical properties are mainly characterized by the shear strength, as seen in Equation (1), where τ is the shear strength (MPa), c is the interlayer bonding force (MPa), σ is the interfacial friction stress (MPa), and φ is the cross-sectional internal friction angle (°).

$$\tau = c + \sigma \tan\varphi \tag{1}$$

As shown in Equation (1), the shear stress between structural layers consists of bonding power and frictional force. The interlayer cementing force generated by the gelled substances in the base materials is the bonding power, whereas the frictional force reflects the friction and extrusion between base materials.

In ABAQUS, the tangential effect between contact planes at each layer is generally characterized through the Coulomb friction model. When the tangential stress is smaller than the critical tangential stress, no interlayer relative slip will occur. The Coulomb friction is expressed in Equation (2), where τ_{crit} is the critical tangential stress (N), μ is the friction coefficient, and p is the normal pressure (N).

$$\tau_{\text{crit}} = \mu p \tag{2}$$

When different construction technologies are applied to the bases, different interlayer bonding states will be presented, so the contact between cement-stabilized magnesium slag–aeolian sand bases should be considered. The bonding state between bases is regarded as a contact state, the interlayer frictional behaviors is simulated through the friction coefficient μ , and contact elements are introduced to simulate the mechanical response of each structural layer. In this study, the contact problem between bases was simulated through surface-to-surface contact.

3.2 Finite element modeling and analysis scheme

3.2.1 Road structure and material parameters

On the basis of the typical structure of asphalt pavements and road construction experiment, the asphalt pavement structure with cement-stabilized magnesium slag–aeolian sand bases was determined (Table 1). The material parameters of the cement-stabilized magnesium slag–aeolian sand mixture were determined according to the indoor test results, whereas other parameters referred to the recommended values in relevant standards, as well as in related literature [29].

Table 1. Road structure and material parameters

Structural layer	Material	Thickness (mm)	Resilient modulus (MPa)	Poisson's ratio	Damping	quality density (kg/m^3)
upper surface	AC-16 asphalt mixture	50	1100	0.25	0.9	2400
lower surface	AC-20 asphalt mixture	70	1400	0.25	0.9	2400
upper base	cement-stabilized magnesium slag–aeolian sand (cement : magnesium slag : aeolian sand = 5 : 60 : 40)	160	1756	0.25	0.8	1968
lower base	cement-stabilized magnesium slag–aeolian sand (cement : magnesium slag : aeolian sand = 5 : 60 : 40)	160	1756	0.25	0.8	1968
subbase	cement-stabilized magnesium slag–aeolian sand (cement : magnesium slag : aeolian sand = 3 : 80 : 20)	200	1564	0.25	0.8	2042
soil subgrade	–	–	60	0.4	0.4	1700

3.2.2 Simulation of construction technologies

On the basis of the theoretical design methods specified in the standards and conventional construction methods, three construction technologies of upper base, lower base, and subbase were planned. (1) Three-layer continuous construction: The lower and upper base courses were directly and continuously paved after the paving of the subbase course; (2) Layered continuous construction: The subbase was initially paved, followed by 7 d of curing and the continuous paving of the lower and upper bases; (3) Layered discontinuous construction: The subbase was initially paved, followed by 7 d of curing and the paving of the lower subbase. The upper subbase was paved after curing for another 7 d. The upper base, lower base, and subbase were regarded as a whole, and a complete continuous model was established as the control group.

When the base courses were discontinuously constructed, the lower base was already hardened after paving, grinding, and curing. Subsequently, the upper base was paved, but an effective bonding layer could not be formed between the upper and lower bases. In case of continuous construction, the upper base was paved immediately after the lower base was paved and grinded before complete hardening. Under the effect of vibration, the lower base mixture and that at the contact part were mutually embedded and squeezed, thereby aggravating the frictional resistance between the upper and lower bases.

Hence, different friction coefficients μ were set to characterize the interaction between contact surfaces. If the overall construction was regarded as continuous contact, then the discontinuous construction was simulated through approximately smooth contact, and μ was taken as 0.1. The continuous construction was simulated through semi-contact, and μ was 1.0 [30]. In addition, the upper surface–lower surface and the soil subgrade–subbase were regarded as a whole, they contacted continuously. The surface and base could be bonded by priming oil to some extent, but an overall structure could not be formed. According to the literature [7], the value of μ between the asphalt surface course and base course was 0.399 – 0.829, so it was taken as 0.6 in this study.

To sum up, the interlayer contact state of the control group and three construction technologies were described as follows: (1) Control group: overall construction, with complete continuity of the upper base, lower base, and subbase; (2) Technology 1: three-layer continuous construction, with the value of μ between the upper and lower bases and that between the lower base and subbase being 1.0; (3) Technology 2: layered continuous construction, with the value of μ between the upper and lower bases being 1.0 and that between the lower base and subbase being 0.1; and (4) Technology 3: layered discontinuous construction, with the value of μ between the upper and lower bases and that between the lower base and subbase being 0.1.

3.2.3 Determination of moving loads

In the current Chinese standards, a double-wheel single-axle load of 100 kN serves as the standard axle load, the single-wheel axle load is F =25 kN, the ground pressure of tires is p =700 kPa, and the center-to-center distance between two wheels is RL =31.95 cm. The contact surface of tires was simplified into a rectangle, whose size was calculated as 156.84 mm × 227.73 mm. Therefore, the rectangular size was approximated as 158 mm × 228 mm and RL as 320 mm.

During modeling, a 4.104 m of load moving belt was set along the load movement direction, each wheel was segmented into three elements along the movement direction, each element was 0.076 m in length, and the load moving belt was divided into 54 elements. The running speed was 20 m/s, and the load was applied by wheels to each element for 0.0038 s during running, that is, each incremental step was 0.0038 s, and the analysis step was 0.2052 s. The traffic load was moving load uniformly distributed in a vertical rectangular shape. The load could be applied by programming DLOAD user subroutine via Fortran language.

3.2.4 Modeling

A 3D 1/2 model was established considering the symmetry between road structure and traffic load. The X-axis was taken as the road width direction (3 m), the Y-axis as the road depth direction (3 m), and the Z- axis as the driving direction (6 m). The vehicle moved along the negative direction of the Z-axis. During mesh generation, the zone of load action was densified, the part close to the zone of load action was divided into fine meshes, and the distant part was divided into coarse meshes. The element type was C3D8R.

As for boundary conditions, all six degrees of freedom on the undersurface were fixed. The two planes perpendicular to the driving direction, namely, Z=0 and Z=3000, were U3=0. The X=0 plane parallel to the driving direction and distant from the load belt was U1=0, and the X=3000 plane close to the load belt was U1=UR2=UR3=0. When the contact property was defined, the normal behavior was set as “hard” contact, the vertical stress and displacement were allowed to continuously transfer between contact layers, and the corresponding friction coefficient was set for tangential behaviors. The final model is shown in Fig. 1.

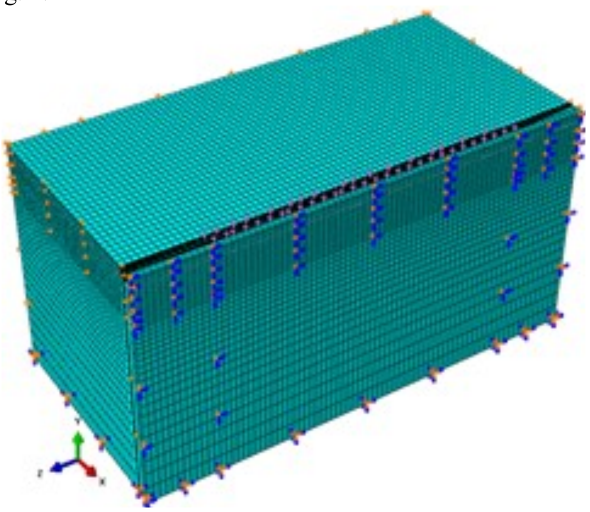

Fig. 1. Structural model of asphalt pavement with cement-stabilized magnesium slag–aeolian sand base courses

3.2.5 Finite element analysis scheme

The main failure modes of asphalt pavements include ruts, fatigue cracking, and shear deformation. When the load moved to the central position of the load belt, the extraction path of mechanical response was a distance range of 1.5 m from the center of the load belt (the distance along the pavement width was positive in forward direction and negative in the negative direction). The vertical displacement, horizontal tensile stress, and maximum shear stress of structural layers were taken as the analysis indexes for the mechanical response of the pavement structure.

4. Results analysis

4.1 Vertical displacement

Fig. 2 displays the curve chart of the changes in the vertical displacements of road surface, base, subbase, and subgrade surface with the distance along the road width in the control group and under the three construction technologies (i.e., their distribution in the road width direction).

As shown in Fig. 2, the vertical displacements on the surface of each structural layer in the control group and under the three construction technologies showed basically identical change laws with the distance along the road width. That is, their distribution characteristics along the road width direction would not be influenced by the change in the interlayer contact state between bases. Under the three construction technologies, the vertical displacement on the road and base surfaces presented an obvious bimodal distribution in the road width direction. In addition, the peak value appeared on the contact surface of tires, whereas those on the subbase and subgrade surface were inclined to a unimodal distribution in the road width direction, where the peak value was distributed in the central area of the load belt. Conversely, the vertical displacement on the surface of each structural layer was the minimum in the event of complete continuity of base and subbase, followed by that under three-layer continuous construction and layered continuous construction, and the vertical displacement was the maximum during layered discontinuous construction. The results revealed that the overall road stiffness was significantly influenced by the interlayer contact state between bases.

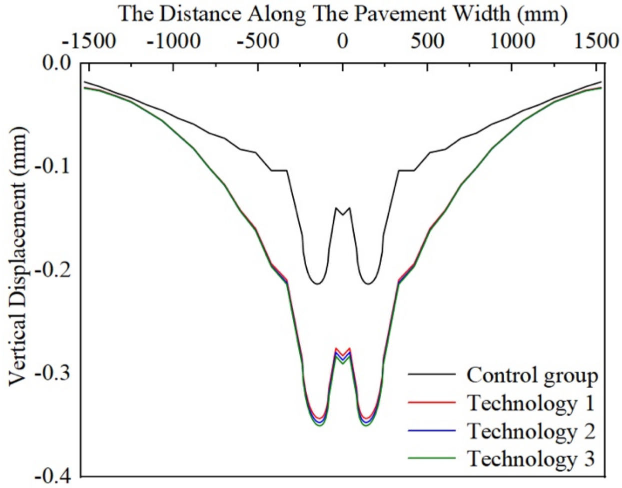

(a)

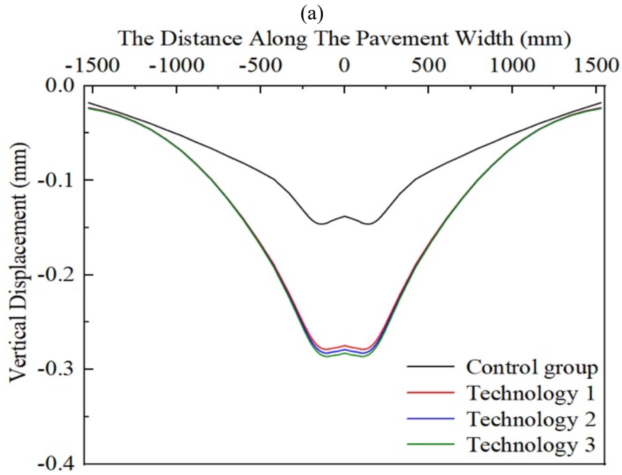

(b)

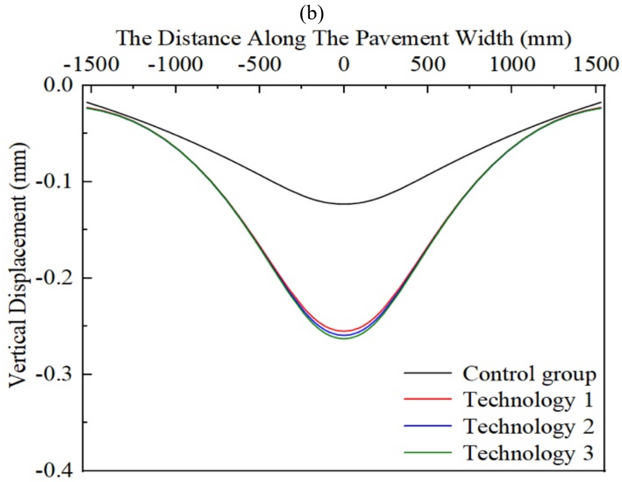

(c)

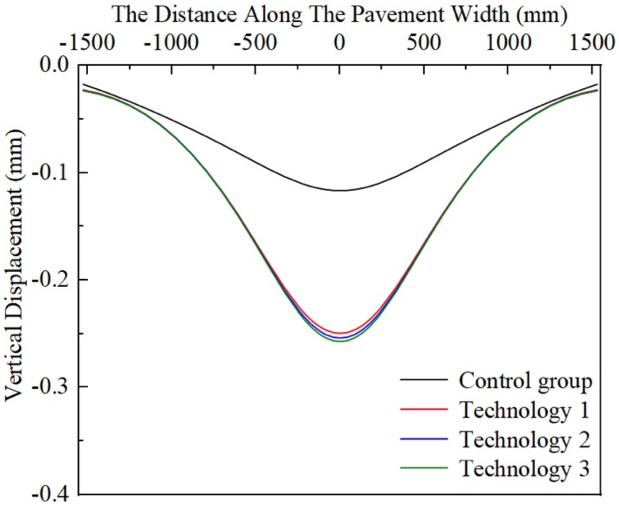

(d)

Fig. 2. Distribution of vertical displacement on the surface of each structural layer. (a) Road surface. (b) Base surface. (c) Subbase surface. (d) Subgrade surface

Table 2 presents the maximum vertical displacement value at each layer. The interlayer contact state between bases influenced the vertical displacement value at each structural layer, but the influencing laws were varied. In comparison with the situation in the control group, the overall maximum vertical displacement value of the road under Technologies 1–3 increased averagely by 62.7%, that in the surface was reduced averagely by 3.7%, that in the base increased averagely by 1.9%, that in the subbase was reduced averagely by 15.4%, and that in the subgrade increased averagely by 117.2%. Under the three construction technologies, the vertical displacement of the subgrade averagely accounted for 73.0% of the overall road displacement, which was far higher than the proportion at other structural layers. This result reflected that no matter what base construction technology was adopted, the subgrade was the primary factor deciding the overall vertical displacement of the asphalt pavement with cement-stabilized magnesium slag–aeolian sand bases.

Table. 2. Maximum vertical displacement value at each structural layer

Group	Vertical displacement value (mm)				
	Overall road	Surface	Base	Subbase	Subgrade
control group	-0.2135	-0.0674	-0.0228	-0.0065	-0.1168
technology 1	-0.3438	-0.0651	-0.0234	-0.0056	-0.2497
technology 2	-0.3476	-0.0650	-0.0231	-0.0053	-0.2542
technology 3	-0.3509	-0.0647	-0.0232	-0.0056	-0.2574

4.2 Horizontal tensile stress

Fig. 3 shows the curve chart of the changes in the horizontal tensile stress at the bottom of each structural layer with the distance along the road width in the control group and under the three construction technologies (i.e., its distribution in the road width direction).

As shown in Fig. 3, the upper surface and the upper base in the control group were mainly subjected to compressive stress, whereas tensile stress played a dominant role at the bottom of other layers. The horizontal tensile stress at the bottom of the upper and lower surfaces presented a bimodal distribution in the road width direction, whereas that at the bottom of the upper base, lower base, and subbase showed a unimodal distribution, with minor fluctua tions. Under the three construction technologies, the tensile stress dominated at the bottom of all structural layers except the bottom of the upper surface, which was prone to compressive stress. In comparison with the situation of complete continuity of base–subbase, the horizontal compressive stress at the bottom of the upper base became tensile stress, which would aggravate the fatigue failure of the pavement to some extent.

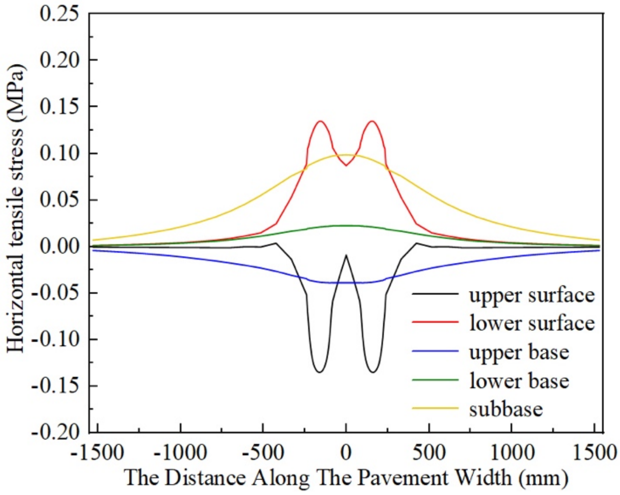

(a)

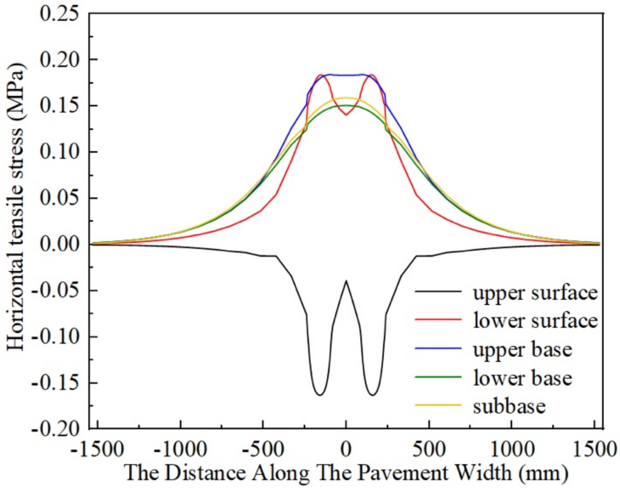

(b)

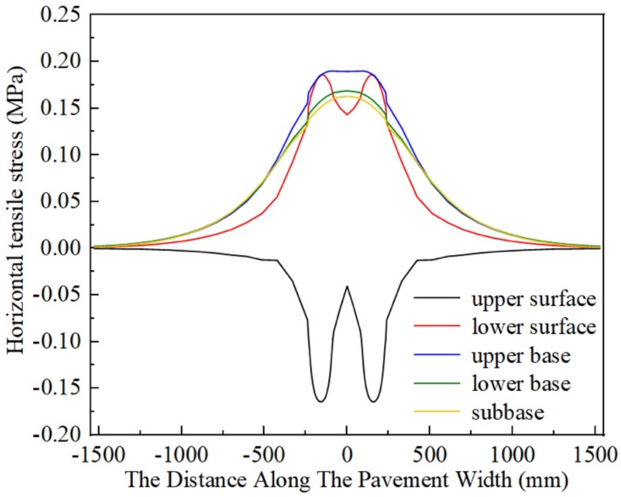

(c)

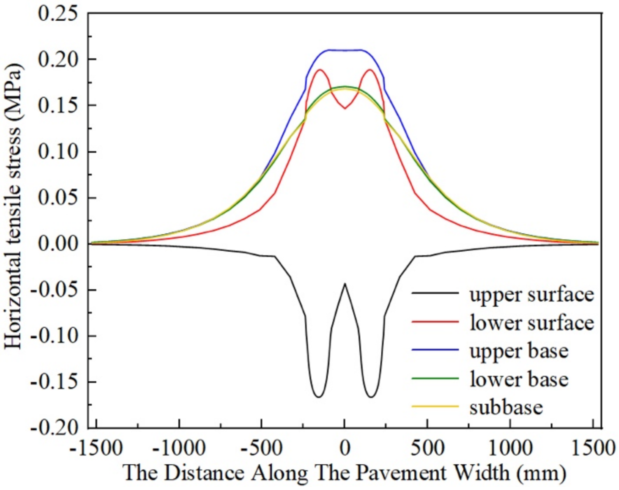

(d)

Fig. 3. Distribution of horizontal tensile stress at the bottom of each structural layer. (a) Control group. (b) Technology 1. (c) Technology 2. (d) Technology 3

Table 3 displays the maximum horizontal tensile stress value at the bottom of each layer. In comparison with the control group, the maximum horizontal tensile stress value at the bottom of the surface under Technologies 1–3 increased averagely by 30.1%, that at the bottom of the base increased averagely by 512.3%, and that at the bottom of the subbase increased averagely by 65.5%. The extent of change was sorted as base>subbase>surface. When the interlayer contact state between the base and subbase turned from a continuous state into a discontinuous state, the horizontal tensile stress value at the bottom of each structural layer was enlarged to different extents, which was especially prominent for the upper and lower bases. Hence, the base structure was more prone to cracks during operation, which would further propagate to the asphalt surface.

Table. 3. Maximum horizontal tensile stress value at the bottom of each structural layer

Group	Horizontal tensile stress value (MPa)				
	Upper surface	**Lower surface**	**Upper base**	**Lower base**	**Subbase**
control group	-0.1348	0.1352	-0.0386	0.0228	0.0990
technology 1	-0.1630	0.1842	0.1845	0.1512	0.1595
technology 2	-0.1642	0.1866	0.1902	0.1689	0.1631
technology 3	-0.1661	0.1896	0.2110	0.1715	0.1690

Among the three construction technologies, the value of μ was large under Technology 1, and the horizontal tensile stress value at the bottom of the upper base was the maximum, followed by that of the subbase and lower base successively. The values of μ under Technologies 2 and 3 were reduced. The horizontal constraint borne by the upper and lower bases was relieved and was free to slide to different extents; thus, the horizontal tensile stress value at the bottom increased. The horizontal stress value at the bottom of the subbase changed slightly because the interlayer contact state between the subbase and subgrade was unchanged.

4.3 Maximum shear stress

Fig. 4 shows the curve chart of the changes in the maximum shear stress at the bottom of each structural layer with the distance along the road width in the control group and under the three construction technologies (i.e., its distribution along the road width direction).

As shown in Fig. 4, under the three construction technologies, the distribution of the maximum shear stress at the bottom of surface along the road width direction was identical with that in the control group, both presenting a bimodal distribution rightly beneath the load belt. The peaking phenomenon of the maximum shear stress at the bottom of surface was especially prominent in comparison with other structural layers. This result indicates that the distribution area of the maximum shear stress was small, which was mainly distributed within a limited range beneath the load belt. In the event of complete continuity of base–subbase, the maximum shear stress at the bottom of base was smaller than that at the bottom of surface, the maximum shear stress at the bottom of the upper and lower bases presented a bimodal distribution, and the peak value was gentle. When the base and subbase were contacted discontinuously, the maximum shear stress value at the bottom of all structural layers, except the upper surface, was enlarged to different extents. In this case, the shear stress was concentrated at the bottom of the upper and lower bases and failed to transfer downward. Thus, the maximum shear stress value at the bottom of the upper base was evidently larger than that at the bottom of the lower base and subbase. In addition, the maximum shear stress value at the bottom of the lower base exceeded that at the bottom of subbase, accompanied by the shift from a smooth bimodal distribution to a unimodal one.

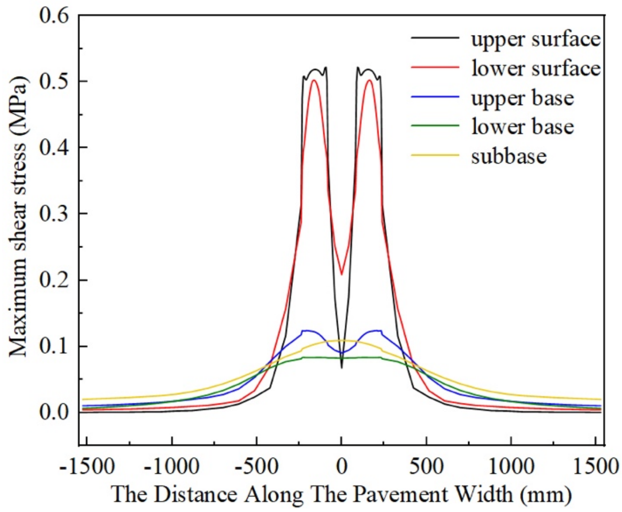

(a)

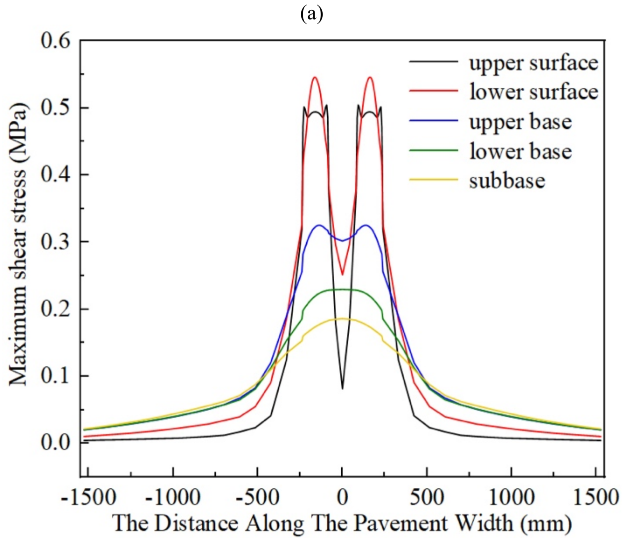

(b)

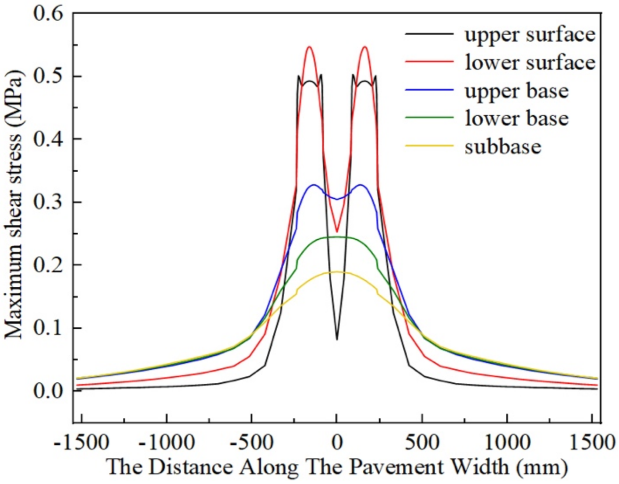

(c)

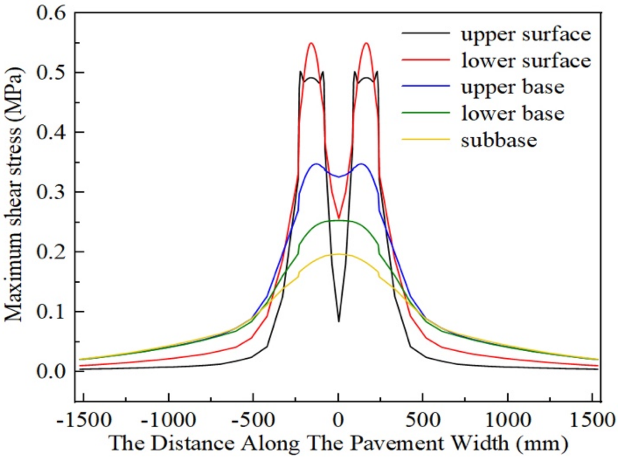

(d)

Fig. 4. Distribution of maximum shear stress at the bottom of each structural layer. (a) Control group. (b) Technology 1. (c) Technology 2. (d) Technology 3

Table 4 shows the maximum shear stress value at the bottom of each structural layer. In comparison with the control group, the maximum shear stress value at the bottom of the upper surface under Technologies 1–3 was reduced averagely by 4.2%, that at the bottom of the lower surface increased averagely by 9.0%, that at the bottom of the base increased averagely by 179.6%, and that at the bottom of the subbase increased averagely by 74.8%. The extent of change was sorted as base>subbase>surface. The results revealed that the discontinuous interlayer contact state between bases would substantially increase the shear stress value at the bonding part of the upper base, lower base, and subbase. Thus, the interlayer contact surface became a weak link in the pavement structure, and the base of the asphalt pavement was more likely to experience shear failure.

Table. 4. Maximum shear stress value at the bottom of each structural layer

Group	Maximum shear stress value (MPa)				
	Upper surface	Lower surface	Upper base	Lower base	Subbase
control group	0.5188	0.5028	0.1244	0.0836	0.1094
technology 1	0.5049	0.5462	0.3255	0.2298	0.1860
technology 2	0.4935	0.5480	0.3286	0.2460	0.1905
technology 3	0.4921	0.5502	0.3478	0.2535	0.1971

4.4 Influencing degree of interlayer contact state

The interlayer contact state between the base and subbase would generate different influences on the vertical displacement, horizontal tensile stress, and maximum shear stress in the structural layers of the pavement structure with cement-stabilized magnesium slag–aeolian sand bases. However, different indexes varied in physical significance and dimension, so their influencing degrees could not be directly compared. Gray relational analysis was adopted in this study in selecting the construction method for cement-stabilized magnesium slag–aeolian sand bases and determining the subsequent key construction technologies and quality control essentials. This approach aims to analyze the influencing degrees of the interlayer contact state on the mechanical response of each pavement structural layer. The comprehensive performance of the three construction technologies was also compared.

Each group of sequences contained 14 factors, including the vertical displacement at the structural layers (i.e., surface, base, subbase, and subgrade), as well as the horizontal tensile stress and maximum shear stress at the bottom of the structural layers (i.e., upper surface, lower surface, upper base, lower base, and subbase; the absolute values are taken in case of negative numbers) recorded as Factors 1–14. The minimum value of mechanical response was regarded as the ideal operation state of the pavement, namely, the minimum value of each factor served as the reference sequence (X_0), and the factor values in the control group and under the three construction factors were taken as the comparison sequences ($X_1 - X_4$, Table 5).

Each sequence was subjected to dimensionless processing through "initialization," and the absolute differences and correlation coefficients (Fig. 5) between comparison sequences were calculated. The greater correlation indicated the greater closeness of this factor value to the optimal value, that is, this factor was influenced by the change in the interlayer contact state to a smaller extent.

Table 5. Numerical values of reference and comparison sequences

Factor	X_0	X_1	X_2	X_3	X_4
1	0.0647	0.0674	0.0651	0.0650	0.0647
2	0.0228	0.0228	0.0234	0.0231	0.0232
3	0.0053	0.0065	0.0056	0.0053	0.0056
4	0.1168	0.1168	0.2497	0.2542	0.2574
5	0.1348	0.1348	0.1630	0.1642	0.1661
6	0.1352	0.1352	0.1842	0.1866	0.1896
7	0.0386	0.0386	0.1845	0.1902	0.2110
8	0.0228	0.0228	0.1512	0.1689	0.1715
9	0.0990	0.0990	0.1595	0.1631	0.1690
10	0.4921	0.5188	0.5049	0.4935	0.4921
11	0.5028	0.5028	0.5462	0.5480	0.5502
12	0.1244	0.1244	0.3255	0.3286	0.3478
13	0.0836	0.0836	0.2298	0.2460	0.2535
14	0.1094	0.1094	0.1860	0.1905	0.1971

As shown in Figure 5, the horizontal tensile stress value at the bottom of the upper and lower bases was influenced to the greatest extent, followed by the maximum shear stress value at the bottom of the upper and lower bases and the vertical displacement value of the subgrade, whereas other factors were influenced slightly. When the bases were under a continuous contact state according to the current specifications, Table 5 indicates that the response value of the horizontal tensile stress at the bottom of bases was considerably smaller than that in case of a discontinuous state. Thus, bases with smaller thickness will pass the base fatigue cracking checking. The discontinuous state of bases, however, conformed more to the actual operation state of the pavement, and the thickness of the base obtained by the model under a continuous state failed to meet practical needs, which was also the reason why the asphalt pavement was prone to all types of damage in the early operation phase.

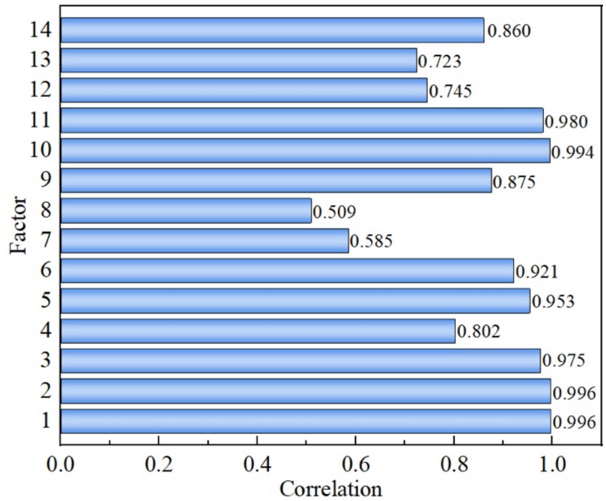

Fig. 5. Correlation of factors

To evaluate and compare the comprehensive performance of the pavement, the mechanical response value in the event of a complete continuous contact state between bases was regarded as the benchmark to calculate the pavement performance index in the control group and that under the three construction technologies. A smaller index represented better performance.

$$C_i = \sum_{k=1}^{14} \frac{x_i(k)}{x_0(k)} \cdot \gamma(k) \tag{3}$$

The performance indexes of each group were acquired through the above equation as C_0 =12.230, C_1 =22.241, C_2 =22.915, and C_3 =23.684. This result indicates that the comprehensive performance index significantly dropped when the bases turned from a complete continuous state into a discontinuous one. In comparison with the situation under Technology 1, the performance index under Technologies 2 and 3 declined by 3.0% and 6.5%, respectively.

To sum up, given the differences between the subbase and base in material compositions, when the three-layer continuous construction is adopted, high requirements will be imposed on the scale of mixing station and field cooperation, accompanied by the large quantity of field construction machineries and personnel, as well as the high cost and difficulty of construction quality control. Hence, the layered continuous construction technology is recommended for cement-stabilized magnesium slag–aeolian sand bases, because it not only can ensure the good mechanical properties of the pavement but also reduce the construction difficulty, save the curing period by 7 d, and save the construction time and economic costs. A discontinuous model should be used in the pavement structural design, or necessary measures specific to bases and subgrades can be taken during construction to avoid early diseases of the asphalt pavement.

5. Conclusions

To ensure that cement-stabilized magnesium slag–aeolian sand base materials can exert good pavement performance in practical engineering, a finite element continuous model of such bases and their contact model under three construction technologies were established in this study. Moreover, the influence of the interlayer contact state among the upper base, lower base, and subbase on the mechanical response of cement-stabilized magnesium slag–aeolian sand bases was analyzed. Finally, the following conclusions could be drawn:

(1) When the interlayer contact state is turned from a continuous state into a discontinuous state, the mechanical response indexes at each structural layer present the following change laws:

The vertical displacement basically shows an unchanged distribution on the surface of each layer, and its value is influenced by different laws. However, the subgrade is always the primary factor deciding the overall vertical displacement of the asphalt pavement under different construction technologies.

The horizontal tensile stress presents a bimodal distribution at the bottom of surface, but it is distributed in the center of the load belt at other layers, and the compressive stress at the bottom of the upper base is transformed into a tensile stress. The horizontal tensile stress value at the bottom of each structural layer increases to different degrees, which is especially prominent in the upper and lower bases, and cracks tend to occur during the operation period.

The maximum shear stress presents a bimodal distribution at the bottom of surface, but the smooth bimodal distribution at the bottom of the lower base is changed into a unimodal distribution. Except that at the bottom of the upper surface course, the maximum shear stress value increases to different extents at other layers, which is especially prominent in the upper and lower bases.

(2) The horizontal tensile stress value at the bottom of the upper and lower bases is influenced, to the greatest extent, by the interlayer contact state between bases, followed by the maximum shear stress value at the bottom of the upper and lower bases and the vertical displacement value in the subgrade, whereas other factors are influenced slightly.

(3) Due to the change in the interlayer contact state, the pavement performance index decreases significantly, which can easily lead to early diseases of the pavement. Given this, a contact model should be used to design the pavement structure. In comparison with the situation under Technology 1, the pavement performance index under Technologies 2 and 3 declines by 3.0% and 6.5%, respectively. Fully considering the pavement performance and construction cost, Technology 2 is recommended, and pertinent measures should be taken in the construction stage.

In this study, the influence of the interlayer contact state between bases on their mechanical response was analyzed to provide a theoretical basis for determining their construction and key technologies. However, the actual operation state of bases can be highly complicated, and this study is not comprehensive enough. Hence, traffic loads can be set in the event of uneven pavement and emergency brake in the follow-up study. In the meanwhile, the numerical simulation results can be verified and corrected through practical observation.

References

1. Qiao, L. D., Yao, Z. Q., Wang, Z. X., Zhang, Z. J., He, L., "Grey entropy analysis of coal gangue on macro and micro properties of concrete". *Journal of Drainage and Irrigation Machinery Engineering*, 40(1), 2022, pp.30-34+54.
2. Li, H. B, Feng, Z. X., Ahmed, A. T., Yombah, M., Cui, C. Y., Zhao, G. J., Guo, P., Sheng, Y. P., "Repurposing waste oils into cleaner aged asphalt pavement materials: A critical review". *Journal of Cleaner Production*, 334, 2022, pp.130230.
3. Wang, S. Y., Xiao, L. G., Zhou, Q., Xu, K., Chen, B. L., Wang, J. F., Wu, Z. Z., "Research and application on magnesium slag". *Advanced Materials Research*, 280, 2011, pp.208-211.
4. Wang, X. B., Yan, X., Li, X. Y., "Environmental risks for application of magnesium slag to soils in China". *Journal of Integrative Agriculture*, 19(7), 2020, pp.1671-1679.
5. Tang, Y. Y., Li, L. B., Wang, C., Mao, W. B., Feng, L., "New progress in reutilization of magnesium slag". *Modern Chemical Industry*, 40(12), 2020, pp.63-67.
6. Lu, X. L., Ding, S. J., Yang, W. Z, Zheng, W. F., "Uplift field load tests on spread foundations in aeolian sand area". *Journal of Water Resources and Architectural Engineering*, 15(5), 2017, pp.20-25.
7. Hu, G., "Impact of interlayer contact state on mechanical eesponse for pavement structures". *Highway*, 60(3), 2015, pp.34-40.
8. Li, H. B., Feng, Z. X., Liu, H., Ahmed, A. T., Zhang, M. M., Zhao, G. J., Guo, P., Sheng, Y. P., "Performance and inorganic fume emission reduction of desulfurized rubber powder/styrene–butadiene–styrene composite modified asphalt and its mixture". *Journal of Cleaner Production*, 364, 2022, pp.132690.
9. Karatag, H., Firat, S., Isik, N. S., "Utilization of steel slag as road base and subbase material". *Journal of Polytechnic*, 23(3), 2019, pp.799-812.
10. Ashfaq, M., Heera, L. M., Moghal, A. A. B., "Influence of lime on the unconfined compressive strength of cnoal gangue". In: *Proceedings of the Indian Geotechnical Conference 2019*, Singapore, Springer, 2021, pp.127-133.
11. Gonawala, R. J., Khapre, S., Kumar, R., Chauhan, K. A., "Suitability of EAF slag and GGBFS mix as cementitious base/subbase layer for low volume road construction". *International Journal of Geotechnical Engineering*, 15(2), 2019, pp.252-258.
12. Pires, P. M., Teixeira, J. E. S. L., Nepomuceno, D. V., Furieri, E. C., "Laboratory and field evaluation of KR slag-stabilized soil for paving applications". *Journal of Materials in Civil Engineering*, 31(9), 2019, pp.04019182.
13. Reinik, J., Irha, N., Koroljova, A., Meriste, T., "Use of oil shale ash in road construction: results of follow-up environmental monitoring". *Environmental Monitoring & Assessment*, 190(2), 2018, pp.59.
14. He, W., Liu, J. F., Yin, P. B., Chen, Y. H., Yang, W. B., Chen, Y. L., Wu, Y. C., "Properties and field tests of industrial ferro-nickel slag for roads". *Chinese Journal of Geotechnical Engineering*, 41(10), 2019, pp.1809-1816.
15. Huang, J. Y., Yang, S. C., Li, S. X., "New way of building black pavement base in western area of Yingkou city". *Liaoning Transportation Technology*, (4), 1994, pp.11-14.
16. Zhao, S. Z., Han, F. L., Wang, Y. G., "Preperation of composite slag sulphoaluminate cement clinker from electrolytic manganese-magnesium". *Bulletin of the Chinese Ceramic Society*, 36(5), 2017, pp.1766-1772+1776.
17. Du, Q., Cui, Z. Z., Zhao, W., Du, F. J., Li, H., "Experimental study on performance of magnesium slag- modified asphalt". *New Building Materials*, 37(2), 2010, pp.58-60+74.
18. Liu, L., Ruan, S. S., Qi, C. C., Zhang, B., Tu, B. B., Yang, Q. X., Song, K., "Co-disposal of magnesium Slag and high-calcium fly ash as cementitious materials in backfill". *Journal of Cleaner Production*, 279, 2021, pp.123684.
19. Song, L. R., Li, B. Y., "Effect of aeolian sand content on mechanical properties and durability of cement stabilized graded macadam". *Bulletin of the Chinese Ceramic Society*, 39(5), 2020, pp.1421-1429.
20. Al-Taie, A. J., Al-Shakarchi, Y. J., Mohammed, A. A., "Investigation of geotechnical specifications of sand dune soil: a case study around Baiji in Iraq". *International Journal of Advanced Research*, 1(6), 2014, pp.208-215.
21. Zhang, Y. L., Liu. X. M., Xu, Y. T., Tang, B. W., Wang, Y. G., Mukiza, E., "Synergic effects of electrolytic manganese residue-red mud-carbide slag on the road base strength and durability properties". *Construction and Building Materials,* 220(SEP.30), 2019, pp.364-374.
22. Jing, H. J., Zhang, J. H., Gao, M., Liu, Q., Wolowiec-Korecka, E., "Base Performances of Cement-Stabilized Magnesium Slag–Aeolian Sand Mixture[J]. *Acta Montanistica Slovaca*, 26(3), 2021, pp.427-443.
23. Hwang, H-S., Ryu, S-W, Oh, J-S., Cho, Y-H., "Investigation of texture effects at interlayer bonding behavior between asphalt concrete (AC) overlay on Portland cement concrete (PCC)". *Canadian Journal of Civil Engineering*, 49(3),2022, pp.412-419.
24. Mazurek, G., Durlej, M., Iwański, M., "Numerical modelling of interlayer adhesion in the layer of recycled material with the use of the Leutner apparatus and computed tomography scanning". *Structure and Environment*, 13(4), 2021, pp.95-103.
25. Saannibe, C. S., "Effect of tack coat and milk lime on the asphalt mix interlayer bond strength". *International Journal of Pavement Research and Technology volume*, 15, 2022, pp.1127-1138.
26. Spadoni, S., Ingrassia, L. P., Paoloni, G., Virgili, A., Canestrari, F., "Influence of geocomposite properties on the crack propagation and interlayer bonding of asphalt pavements". *Materials*, 14(18), 2021, pp.5310.
27. Wang, X. T., Ma, X. L., "Responses of semi-rigid base asphalt pavement with interlayer contact bonding model". *Advances in Civil Engineering*, 2020.
28. Wu, S. H., Chen, H. X., Zhang, J. P., Zhang, Z. H., "Effects of interlayer bonding conditions between semi-rigid base layer and asphalt layer on mechanical responses of asphalt pavement structure". *International Journal of Pavement Research and Technology*, 10(3), 2017, pp.274-281.
29. Zhou, X. Y., Ma, B., Tian, X. Y., Wang, X Q., "Value of compressive resilient modulus of asphalt mixture in surface layer". *Journal of Jiangsu University (Natural Science Edition)*, 38(5), 2017, pp.615-620.
30. Liang, C. Y., Ma, J. C., Tan, G. J., Xu, X., Zhang, L. D., Luan, H., "Influence of interlayer state of cement stabilized macadam on mechanical response of pavement structure". *Journal of Jilin University: Engineering and Technology Edition*, 52(5), 2022, pp.1063-1070.